GeoAmericas2020
4th PAN AMERICAN CONFERENCE ON GEOSYNTHETICS
26-29 APRIL 2020 • RIO DE JANEIRO • BRAZIL

A simple probabilistic approach for internal stability analysis and design of geosynthetic reinforced soil walls

R.J. Bathurst, GeoEngineering Centre at Queen's-RMC, Royal Military College, Kingston, Canada

ABSTRACT

This paper explains simple probabilistic analysis and design for tensile strength and pullout internal stability limit states for geosynthetic reinforced soil walls. The general approach uses a closed-form solution for reliability index which is easily implemented in a spreadsheet and thus eliminates the need for Monte Carlo simulation. A novel feature of the formulation is that it includes uncertainty in the calculation of nominal values which is consistent with the notion of level of understanding that appears in the Canadian Highway Bridge Design Code, and variability in the underlying accuracy of the load and resistance models that appear in each limit state equation using bias statistics. Here, bias is the ratio of observed value to predicted value using closed-form solutions for load and resistance terms. A design example based on a constructed geogrid reinforced soil wall is used to demonstrate the general approach.

1. INTRODUCTION

Geotechnical foundation engineering, including design of geosynthetic reinforced soil walls (or mechanically stabilized earth (MSE) walls) is moving towards reliability-based analysis and design where margins of safety for limit states are expressed in probabilistic terms (or reliability index). Margins of safety quantified in probabilistic terms are more informative and more intuitive than margins of safety expressed as a factor of safety in deterministic design practice.

Figure 1 shows the notional relationship between true (operational) factor of safety and probability of failure. Here Q_m is measured (observed) load and R_m is measured (observed) resistance. Both quantities have some uncertainty and thus the distributions for Q_m and R_m can be described by frequency distributions located about mean values of measured load and resistance, $\bar{Q}_m$ and $\bar{R}_m$, respectively . The ratio of $\bar{R}_m$ and $\bar{Q}_m$ values can be understood to be the operational (true) factor of safety OFS = $\bar{R}_m / \bar{Q}_m$. As the difference between $\bar{R}_m$ and $\bar{Q}_m$ increases, the true factor of safety increases and the overlap between distributions increases. The area of overlap is notionally related to probability of failure, P_f. The disadvantage of deterministic design practice is that the same factor of safety may have different uncertainty (spread) in Q_m and R_m and thus different probabilities of failure.

The transformation from nominal resistance (R_n) to measured resistance (R_m) and from nominal load (Q_n) to measured load (Q_m) is made by multiplying each nominal value by a corresponding bias value denoted as λ_R and λ_Q, respectively; hence, $Q_m = \lambda_Q\ Q_n$ and $R_m = \lambda_R\ R_n$. If there is no difference between calculated nominal values and measured values then OFS = $F_n = R_n/Q_n$; the quantity F_n is familiar to geotechnical engineers as the classical deterministic factor of safety for a given limit state. The likelihood that nominal and measured load values and nominal and measured resistance values are the same for soil-structure interaction problems, including internal limit states for geosynthetic MSE walls, is vanishingly small.

Simple linear limit states with a single load term can be expressed as:

$$g = \frac{\lambda_R R_n}{\lambda_Q Q_n} - 1 \qquad [1]$$

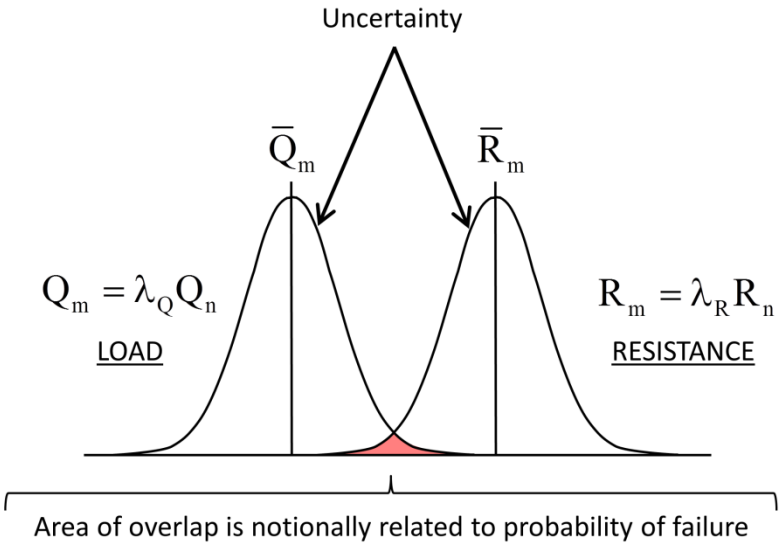

Figure 1. Frequency distributions for measured load (Q_m) and measured resistance (R_m)

If bias values are also assigned uncertainty expressed by a frequency distribution function, then the probability of failure of a limit state is $P_f = P(g < 0)$. The probability of failure can be computed by sampling distributions for λ_Q , Q_n , λ_R and R_n many times, and dividing the number of times that $g < 0$ by the total number of trials (realizations). This is called Monte Carlo (MC) simulation. However, MC simulation may be tedious and many realizations may be required to compute a confident estimate of P_f for cases with low probabilities of failure. Furthermore, there are potential correlations between variables which may have to be accounted for during MC simulation. The influence of these correlations can play out in ways that are not easily detectable by simply counting the number of $g < 0$ occurrences.

Fortunately, there is a closed-form solution for reliability index (β) that can be used to estimate the margin safety in probabilistic terms for the case of simple linear limit state functions with a single load term (Q_n) and all bias and nominal values are lognormally distributed (the typical case); specifically (Bathurst and Javankhoshdel 2017):

$$\beta = \frac{\ln\left[\left(\frac{\mu_{\lambda R}\mu_{Rn}}{\mu_{\lambda Q}\mu_{Qn}}\right)\sqrt{\frac{(1+COV_{Qn}^2)(1+COV_{\lambda Q}^2)}{(1+COV_{Rn}^2)(1+COV_{\lambda R}^2)}}\right]}{\sqrt{\ln\left[\frac{(1+COV_{Qn}^2)(1+COV_{\lambda Q}^2)(1+COV_{Rn}^2)(1+COV_{\lambda R}^2)(1+\rho_R COV_{Rn} COV_{\lambda R})^2 (1+\rho_Q COV_{Qn} COV_{\lambda Q})^2}{(1+\rho_n COV_{Rn} COV_{Qn})^2}\right]}} \quad [2]$$

This equation follows from basic probability theory. All assumptions and full details of its derivation can be found in the appendix to the paper by Bathurst and Javankhoshdel (2017). Parameters μ_{Rn}, μ_{Qn}, $\mu_{\lambda R}$ and $\mu_{\lambda Q}$ are mean values of nominal resistance and load values (R_n and Q_n), and resistance and load bias values (λ_R and λ_Q), respectively. Their corresponding coefficients of variation (COV) are denoted as COV_{Rn}, COV_{Qn}, $COV_{\lambda R}$ and $COV_{\lambda Q}$. The nominal resistance value (R_n) and nominal load value (Q_n) used at time of design in the limit state design equations are equivalent to μ_{Rn} and μ_{Qn} in the above equation.

The COV values for nominal load and resistance values (Q_n and R_n) capture the total uncertainty in the magnitude of nominal values used at time of design from all sources. For example, there is always some uncertainty in the value of friction angle and unit weight that appear in the load and pullout equations introduced later. However, the sources of uncertainty can extend to the applicability of the load and resistance models to project-specific conditions. In Canadian load and resistance factor design (LRFD) foundation practice, the concept of level of understanding has been adopted (CSA 2019). The magnitude of resistance factor used in a limit state design equation in the Canadian LRFD code increases as level of understanding moves from low to high. Level of understanding increases with increasing amount and quality of project materials data, greater experience of the designer with the candidate MSE wall technology, and decreases with increasing complexity of the project and so on. The three levels of understanding that appear in the Canadian code are used to reward

design engineers (and their clients) with more cost effective design solutions as more effort is expended to increase project level of understanding. Stated alternatively, this scheme encourages engineers to collect more site information and to carry out more material property testing.

In order to quantify level of understanding in reliability-based analysis and design, Bathurst et al. (2017) mapped COV of nominal values equal to 0.1, 0.2 and 0.3 to high, typical and low levels of understanding, respectively. These values are used in the calculations that appear later in the paper. The exception is the tensile rupture limit state where COV_{Rn} = 0 because the nominal allowable tensile strength of the reinforcement (T_{al}) used at time of design is prescribed based on project conditions. The uncertainty (or variability) in allowable tensile capacity of the reinforcement is captured entirely by the spread in bias values (i.e. $COV_{\lambda R}$) that is computed from variability in tensile strength at end of design life.

The operational factor of safety introduced earlier appears in the numerator of Equation 2 as:

$$OFS = \frac{\mu_{\lambda R}\mu_{Rn}}{\mu_{\lambda Q}\mu_{Qn}} = \frac{\mu_{\lambda R}}{\mu_{\lambda Q}} \times F_n \qquad [3]$$

Inspection of this equation shows that the true average operational factor of safety is different from the nominal factor of safety as mentioned earlier. Typically, OFS > F_n because resistance models often under-estimate resistance capacity and/or load models tend to over-estimate actual loads.

Parameters ρ_R and ρ_Q in Equation 2 are Pearson's correlation coefficients between variables R_n and λ_R, and between Q_n and λ_Q, respectively, and represent bias dependencies with nominal values. Stated alternatively, these correlations capture the case where model accuracy (i.e. bias) varies with the magnitude of the computed nominal value.

Parameter ρ_n is the correlation coefficient between R_n and Q_n and is called nominal correlation following the terminology introduced by Lin and Bathurst (2018).

The link to probability of failure is $P_f = 1 - \Phi(\beta)$ where $\Phi(\beta)$ is the standard normal cumulative distribution function (NORMSDIST(β) in Excel). The relationship between probability of failure and reliability index is shown in Figure 2.

The ratio of the mean of nominal resistance and mean of nominal load is assumed equal to the nominal factor of safety F_n introduced earlier (i.e. $F_n = \mu_{Rn}/\mu_{Qn} = R_n/Q_n$).

Equation 2 can be written as:

$$\beta = A \times \ln(F_n) + B \qquad [4]$$

where A and B are constant values that are collections of statistical quantities in Equation 2. Equation 4 shows

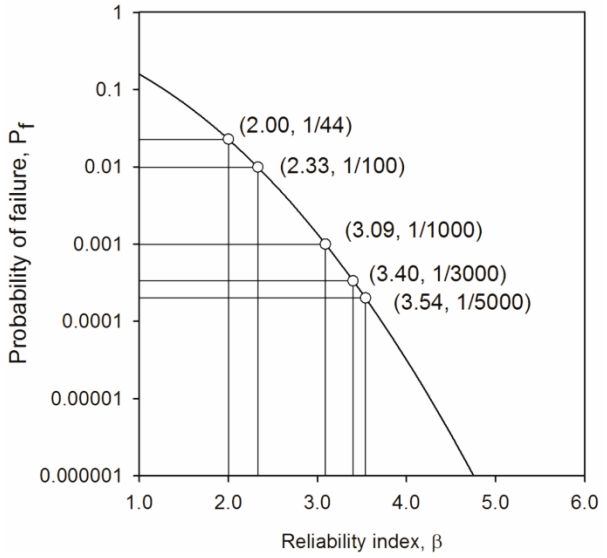

Figure 2. Probability of failure versus reliability index

that there is a log-linear relationship between reliability index β and the nominal factor of safety. By increasing the nominal factor of safety at time of design and keeping all other quantities the same, the margin of safety expressed as reliability index or probability of failure (i.e. $P_f = 1 - \Phi(\beta)$) also increases. While this is expected, Equation 4 (or equivalently Equation 2) has the advantage of providing a quantitative link between deterministic factor of safety design practice and margins of safety expressed in a probabilistic framework.

2. INTERNAL LIMIT STATES

In this paper, internal stability limit states for tensile strength (rupture) and pullout modes of failure are investigated. The geometry and parameters that correspond to these limit states are shown in Figure 3.

2.1 Tensile load

The calculation of nominal load (T_{max}) is based on the Simplified Stiffness Method (Allen and Bathurst 2015, 2018) which has been adopted in the USA AASHTO (2020) LRFD specifications and has the general form:

$$T_{max} = f(H, \Phi_{fs}, S_v, z, \phi, \sigma_v, J) \quad [5]$$

Here, T_{max} is the maximum tensile load in a reinforcement layer under operational conditions and is expressed in units of force per unit running length of wall face (e.g. kN/m). Other terms are H = height of wall, Φ_{fs} = facing stiffness factor, S_v = tributary area of each reinforcement layer, z = depth below crest of the wall, ϕ = peak friction angle of the soil, σ_v = vertical stress due to soil self-weight (γ) plus any uniformly distributed surface surcharge q (i.e. $\sigma_v = \gamma z + q$), and J = secant stiffness value at 2% strain and 1000 h for geotextiles and geogrids (Allen and Bathurst 2015) and 1% strain and 1000 h for polyester straps (Miyata et al. 2018).

2.2 Tensile strength

The ultimate tensile strength (rupture) capacity of the reinforcement is taken as the long-term allowable strength and is computed as (AASHTO 2020):

$$T_{al} = \frac{T_{ult}}{RF} = \frac{T_{ult}}{RF_{ID} \times RF_{CR} \times RF_D} \quad [6]$$

The numerator is a reference laboratory ultimate tensile strength (T_{ult}) that is reduced by factors that account for loss of strength over the design life of the reinforcement due to installation damage (RF_{ID}), creep (RF_{CR}) and degradation (durability) mechanisms (RF_D). Parameter RF is combined reduction factor.

2.3 Pullout

The ultimate pullout capacity (P_c) in this paper is computed using the current AASHTO (2020) model.

$$P_c = 2F^* \alpha L_e \sigma_v R_c \quad [7]$$

Here, F* = coefficient of interaction (dimensionless) = (2/3) tan ϕ, α = 0.8, L_e = anchorage length within the passive zone (Figure 3), and R_c = reinforcement coverage length and is taken as R_c = 1 for continuous reinforcement layers (e.g. the wall case study to follow).

3. EXAMPLE

The example wall case used to demonstrate the calculation of β is taken from Bathurst et al. (2019a,b) and Allen and Bathurst (2014, 2018). The wall geometry and geogrid reinforcement arrangement are shown in Figure 4. Material properties are summarized in Table 1. The reinforcement properties correspond to the least

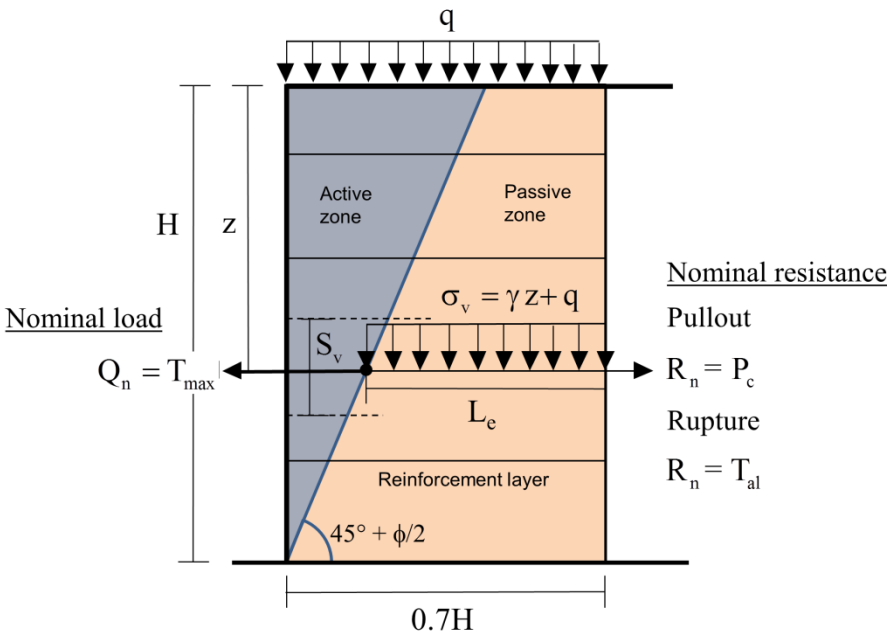

Figure 3. Internal limit states for tensile strength (rupture) and pullout for geosynthetic MSE wall

stiff high density polyethylene (HDPE) geogrid reinforcement material in the geogrid product line that was available at the time the wall was designed.

4. RESULTS

In the analyses carried out in this paper, $\rho_n = 0$ for the rupture limit state because nominal load values and nominal resistance values are sampled from independent populations. For the pullout limit state the soil material properties and their statistical characteristics are the same for the load equation associated with the active wedge in Figure 3 and the pullout equation associated with the passive zone. Hence, $\rho_n \neq 0$ and will vary with changes in the distributions for friction angle and unit weight assumed at the location of each reinforcement layer as demonstrated by Lin and Bathurst (2018). Since P_c will increase with increasing ϕ while T_{max} will decrease with increasing ϕ, a negative nominal correlation is expected between load and resistance values for the pullout limit state. The maximum possible negative value is $\rho_n = -1$ which also gives the most conservative

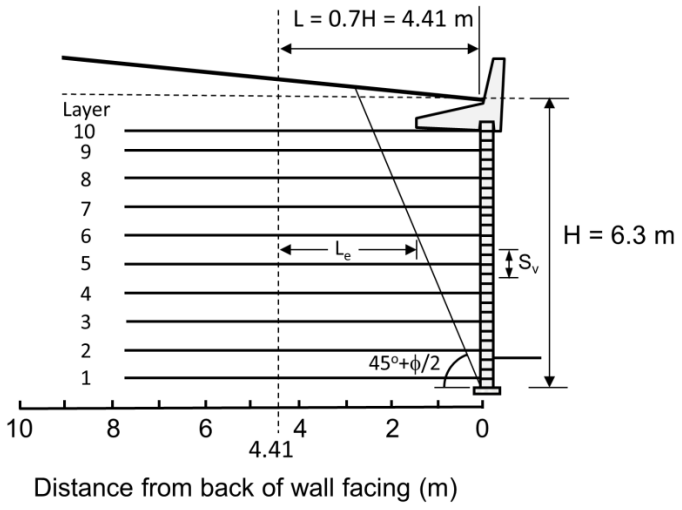

Figure 4. Example geogrid MSE wall (after Allen and Bathurst 2014)

Table 1. Material properties for example wall from Allen and Bathurst (2018)

Parameter	Value
Soil friction angle, ϕ (^{o})	38
Bulk soil unit weight, γ (kN/m^3)	20.4
Soil cohesion (kPa)	0
Equivalent uniform surcharge pressure, S (m)	4.3 kPa
Thickness of the facing column (m)	0.305
Tributary vertical spacing of reinforcement layers, S_v (m)	1 for the top layer; 0.4 for the bottom layer; and 0.6 for other layers
Ultimate tensile strength, T_{ult} (kN/m)	24
Reduction factor, RF	3.6
Allowable tensile load (strength) at end of design life, T_{al} (kN/m)	6.7
Reinforcement stiffness, J (kN/m)	128

outcome (smallest value for β when all other parameters remain unchanged). Inspection of the last parenthetical term in the denominator of Equation 2 reveals why ρ_n = -1 will give the most conservative β outcome. This value is used in the calculations to follow for the pullout limit state. A deeper treatment of this issue can be found in the paper by Bathurst et al. (2019b). Bias statistics for the load and resistance models used in this example are summarized in Table 2.

Results of β calculations using Equation 2 are summarized in Table 3 for the tensile strength limit state and in Table 4 for the pullout limit state. Figures 5 and 6 show plots of β and P_f with depth for the tensile strength limit state and pullout limit state, respectively. The data plots correspond to the three levels of understanding discussed earlier. Note that for the tensile strength limit state, COV_{Rn} = 0 as explained earlier. Superimposed on the figures are target reliability index values of β = 2.33 (P_f = 1/100), 3.09 (P_f = 1/1000) and 3.54 (P_f = 1/5000). A minimum reliability index value of β = 2.33 is recommended for the internal limit states for MSE walls because these systems are highly strength redundant (Allen et al. 2005); if one layer fails the other layers can compensate. The larger target β values corresponding to P_f = 1/1000 and 1/5000 have been recommended for single pile shafts and footings, respectively.

The following observations can be made from Tables 3 and 4 and the plots in Figures 5 and 6:

1. As level of understanding increases, the level of safety described by β and P_f increases.
2. The minimum target β = 2.33 is satisfied for all layers regardless of level of understanding.
3. The lowest margins of safety for the tensile strength limit state are in the bottom half of the wall.

Table 2. Summary of bias statistics and bias dependency values for load and resistance models for geogrid reinforced soil walls constructed with granular soil (from Bathurst et al. 2019b)

Model	Model equation	Number of data points	Mean of bias	COV of bias	Bias dependency	Data source
Load model (Allen and Bathurst 2015)	Equation 5	96	$\mu_{\lambda Q}$ = 0.96	$COV_{\lambda Q}$ = 0.36	ρ_Q = 0.09	Allen and Bathurst (2015)
Pullout model (AASHTO 2020)	Equation 7	318	$\mu_{\lambda R}$ = 2.23	$COV_{\lambda R}$ = 0.55	ρ_R = -0.46	Huang and Bathurst (2009)
Tensile rupture (AASHTO 2020)	Equation 6	N/A	$\mu_{\lambda R}$ = 1.10	$COV_{\lambda R}$ = 0.10	ρ_R = 0	Bathurst et al. (2011)

4. The lowest margin of safety for the pullout limit state is for the layer at the top of the wall.
5. For many of the layers, the computed margin of safety is very large and well beyond minimum levels recommended for non-redundant geotechnical foundation elements.

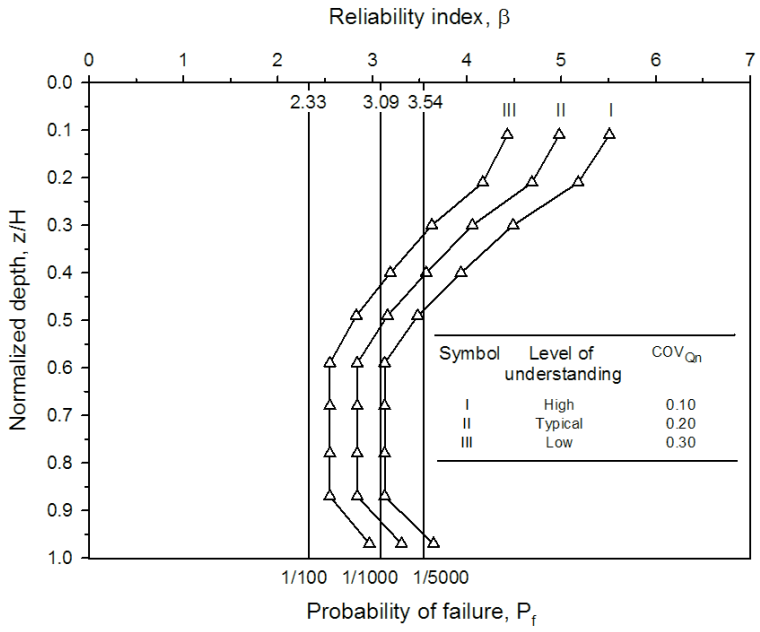

Figure 5. Reliability index for tensile strength limit state (COV_{Rn} = 0)

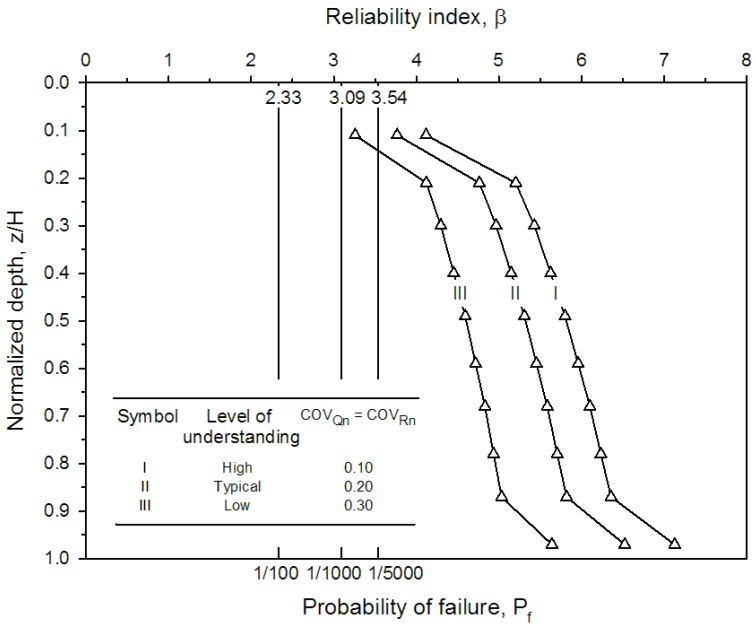

Figure 6. Reliability index for pullout limit state

Observations 3 and 4 are consistent with expectations by experienced MSE wall designers for walls with simple geometry and reinforcement arrangements as in this example.

Figure 7 shows operational factor of safety plotted against nominal factor of safety for both limit states. The relationships are linear as expected from Equation 3. For both limit states the nominal factor of safety is large and the OFS is even larger. The true operational factor of safety is about 15% higher for the tensile strength limit state and larger by a factor of 2.3 for the pullout limit state.

Figure 8 and Figure 9 show reliability index plotted against nominal factor of safety. The relationships are log-linear as expected from Equation 4. As level of understanding increases, reliability index increases for the same nominal factor of safety. Even for the reinforcement layer with lowest nominal factor safety in Figure 8, the margin of safety in terms of reliability index is well above the minimum target value of β = 2.33 corresponding to

Table 3. Tensile strength limit state results for all reinforcement layers (COV_{Rn} = 0)

Layer	Depth, z (m)	Q_n (kN/m)	R_n (kN/m)	F_n	OFS	Reliability index, β		
						Level of understanding		
						High	Typical	Low
						COV_{Qn} = 0.1	COV_{Qn} = 0.2	COV_{Qn} = 0.3
10 (Top)	0.7	1.0	6.7	6.8	7.8	5.51	4.98	4.43
9	1.3	1.1	6.7	6.0	6.9	5.18	4.69	4.17
8	1.9	1.5	6.7	4.6	5.3	4.49	4.06	3.63
7	2.5	1.8	6.7	3.7	4.3	3.94	3.57	3.19
6	3.1	2.1	6.7	3.1	3.6	3.48	3.16	2.83
5	3.7	2.5	6.7	2.7	3.1	3.13	2.84	2.55
4	4.3	2.5	6.7	2.7	3.1	3.13	2.84	2.55
3	4.9	2.5	6.7	2.7	3.1	3.13	2.84	2.55
2	5.5	2.5	6.7	2.7	3.1	3.13	2.84	2.55
1	6.1	2.0	6.7	3.4	3.8	3.65	3.31	2.97

P_f = 1/100. For the pullout limit state, the data in Figure 9 show that the nominal factor of safety values are very large and the corresponding β values are even larger. It can be concluded that for this example wall, there are adequate margins of safety for both limit states expressed in deterministic and probabilistically frameworks.

5. CONCLUSIONS

This paper explains simple probabilistic analysis and design for two internal stability limit states for geosynthetic MSE walls. The general approach uses a closed-form solution for reliability index which is easily implemented in a spreadsheet. While the calculations using this formulation can be done to the same practical accuracy using

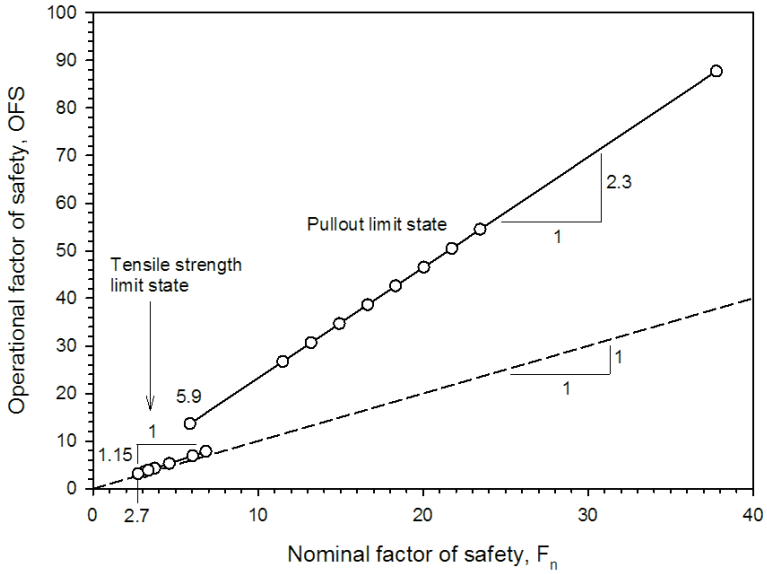

Figure 7. Operational factor of safety versus nominal factor of safety

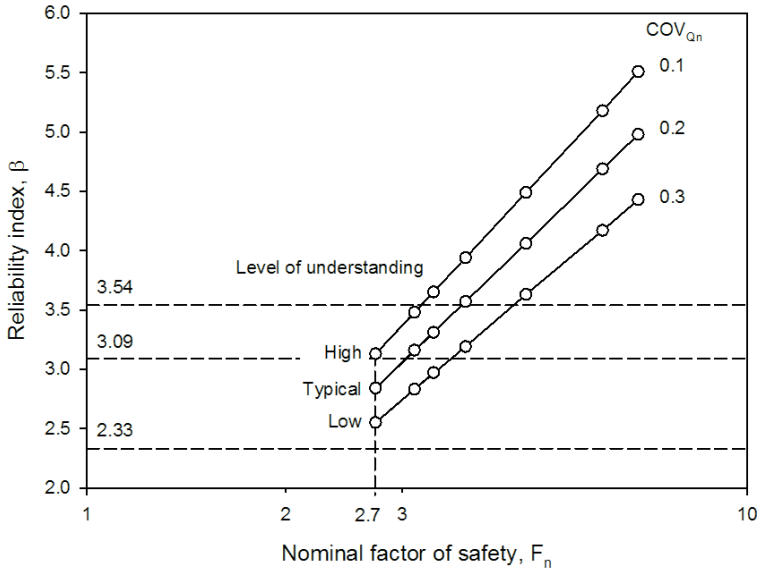

Figure 8. Reliability index versus nominal factor of safety for tensile strength limit state (COV_{Rn} = 0)

conventional MC simulation, the advantage of the closed-form solution is that by inspection it can provide insight on how different statistical quantities influence the magnitude of β. A novel feature of the formulation is that it includes uncertainty in the choice of nominal values and variability in the underlying accuracy of the load and resistance models that appear in each limit state equation using bias statistics. The quantitative effects of selecting different COV of nominal values on β outcomes can be seen as an approach to inject human judgement into the quantitative assessment of probabilistic margins of safety.

Due to space constraints, details on how bias statistics can be gathered and treated could not be presented. The reader is directed to previously cited papers for these details.

The concepts in this paper are general and can be applied to any soil-structure interaction problem that can be expressed by a simple linear limit state performance function with one load term, and for which bias statistics are available.

The general approach explained in this paper provides the MSE wall designer with a tool to make design decisions based on reliability index (or equivalently, probability of failure) which is strongly informative. Nevertheless, the general approach can also be viewed as a complementary approach to traditional factor of safety and LRFD methods for internal stability design of reinforced soil walls.

REFERENCES

Allen, T.M. and Bathurst, R.J. (2014). Design and performance of a 6.3-m-high block-faced geogrid wall designed using the K-stiffness Method. Journal of Geotechnical and Geoenvironmental Engineering 140(2): 04013016.

Allen, T.M. and Bathurst, R.J. (2015). An improved simplified method for prediction of loads in reinforced soil walls. Journal of Geotechnical and Geoenvironmental Engineering 141(11): 04015049.

Allen, T.M. and Bathurst, R.J. (2018). Application of the Simplified Stiffness Method to design of reinforced soil walls. Journal of Geotechnical and Geoenvironmental Engineering 144(5): 04018024.

Allen, T.M., Nowak, A.S. and Bathurst, R.J. (2005). Calibration to determine load and resistance factors for geotechnical and structural design. Transportation Research Board Circular E-C079, Washington, DC, 93 p.

AASHTO. (2020). LRFD Bridge Design Specifications, 9th Ed., American Association of State Highway and Transportation Officials (AASHTO), Washington, DC, USA. (in press).

Bathurst, R.J., Allen, T.M., Lin, P. and Bozorgzadeh, N. (2019a). LRFD calibration of internal limit states for geogrid MSE walls. Journal of Geotechnical and Geoenvironmental Engineering 145(11): 04019087.

Bathurst, R.J., Huang, B. and Allen, T.M. (2011). Analysis of installation damage tests for LRFD calibration of reinforced soil structures. Geotextiles and Geomembranes 29(3): 323-334.

Bathurst, R.J. and Javankhoshdel, S. (2017). Influence of model type, bias and input parameter variability on reliability analysis for simple limit states in soil-structure interaction problems. Georisk 11(1): 42-54.

Bathurst, R.J., Lin, P. and Allen, T.M. (2019b). Reliability-based design of internal limit states for mechanically stabilized earth walls using geosynthetic reinforcement. Canadian Geotechnical Journal 56(6): 774-788.

CSA. (2019). Canadian Highway Bridge Design Code. CAN/CSA-S6-19. Canadian Standards Association (CSA), Mississauga, Ontario, Canada.

Huang, B. and Bathurst, R.J. (2009). Evaluation of soil-geogrid pullout models using a statistical approach. Geotechnical Testing Journal 32(6): 489-504.

Lin, P. and Bathurst, R.J. (2018). Influence of cross-correlation between nominal load and resistance on reliability-based design for simple linear soil-structure limit states. Canadian Geotechnical Journal 55(2): 279-295.

Miyata, Y., Bathurst, R.J. and Allen, T.M. (2018). Evaluation of tensile load model accuracy for PET strap MSE walls. Geosynthetics International 25(6): 656-671.

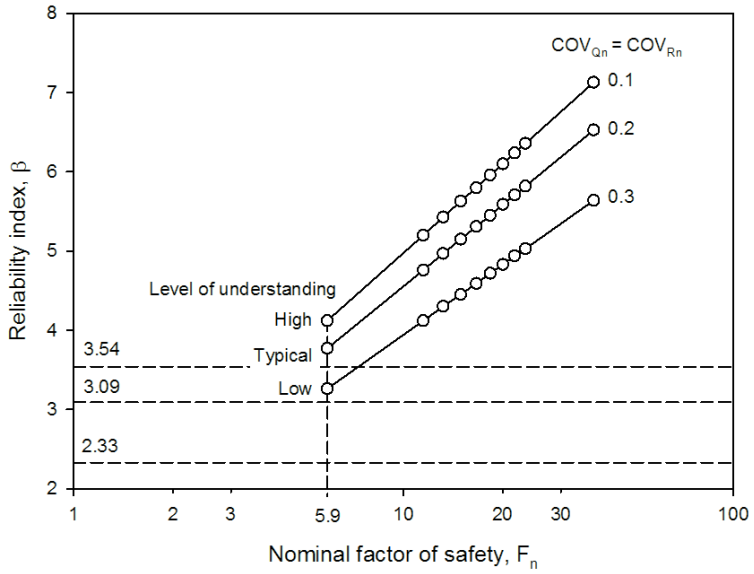

Figure 9. Reliability index versus nominal factor of safety for pullout limit state

Table 4. Pullout limit state results for all reinforcement layers (COV_{Rn} = COV_{Qn})

Layer	Depth, z (m)	Q_n (kN/m)	R_n (kN/m)	F_n	OFS	Reliability index, β		
						Level of understanding		
						High	Typical	Low
						COV_{Qn} = 0.1	COV_{Qn} = 0.2	COV_{Qn} = 0.3
10 (Top)	0.7	4.4	26.0	5.9	13.6	4.12	3.77	3.26
9	1.3	4.4	50.6	11.5	26.7	5.20	4.76	4.12
8	1.9	6.2	81.2	13.2	30.7	5.43	4.97	4.30
7	2.5	7.9	117.8	14.9	34.7	5.63	5.15	4.45
6	3.1	9.6	160.3	16.6	38.6	5.80	5.31	4.59
5	3.7	11.4	208.9	18.3	42.6	5.96	5.45	4.72
4	4.3	13.1	263.3	20.0	46.6	6.10	5.59	4.83
3	4.9	14.9	323.8	21.7	50.5	6.24	5.71	4.94
2	5.5	16.6	390.2	23.5	54.5	6.36	5.82	5.03
1	6.1	12.3	462.6	37.8	87.7	7.13	6.53	5.64